Environmental Science Nano

Accepted Manuscript

This is an *Accepted Manuscript*, which has been through the Royal Society of Chemistry peer review process and has been accepted for publication.

Accepted Manuscripts are published online shortly after acceptance, before technical editing, formatting and proof reading. Using this free service, authors can make their results available to the community, in citable form, before we publish the edited article. We will replace this *Accepted Manuscript* with the edited and formatted *Advance Article* as soon as it is available.

You can find more information about *Accepted Manuscripts* in the Information for Authors.

Please note that technical editing may introduce minor changes to the text and/or graphics, which may alter content. The journal's standard Terms & Conditions and the Ethical guidelines still apply. In no event shall the Royal Society of Chemistry be held responsible for any errors or omissions in this *Accepted Manuscript* or any consequences arising from the use of any information it contains.

ROYAL SOCIETY OF CHEMISTRY

rsc.li/es-nano

Graphical Abstract:

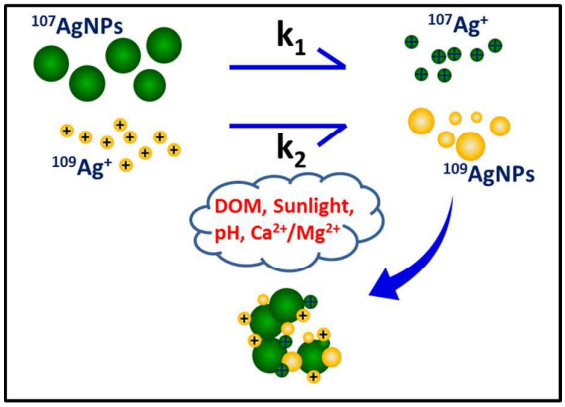

The double stable isotope labeling method (^{107}AgNPs and $^{109}AgNO_3$) was used to track transformation kinetics of AgNPs and Ag^+ in aquatic environments.

Environmental Science: Nano Accepted Manuscript

Nano Impact Statement

With the ongoing commercialization of silver nanoparticles (AgNPs), their release to the environment will considerably increase. AgNPs are highly dynamic, and the fate of AgNPs in the aquatic system is still largely unknown, especially the transformation between AgNPs and Ag^+, which remains a choke point in rational estimating their potential risks. In this study, double stable isotope labeling method was used to monitor the transformation kinetics of AgNPs and Ag^+ in aquatic environments. It was demonstrated that transformation between AgNPs and Ag^+ was complicated, and was affected by a number of environmental factors such as sunlight, dissolved organic matter, solution pH, temperature, and divalent cations. The speciation variation of silver may significantly impact the toxicity and bioavailability of AgNPs. Therefore, more realistic conditions are highly demanded when assessing the environmental hazards of AgNPs.

Environmental Science: Nano Accepted Manuscript

Transformation Kinetics of Silver Nanoparticles and Silver Ions in Aquatic Environments Revealed by Double Stable Isotope Labeling

Sujuan Yu, Yongguang Yin, Xiaoxia Zhou, Lijie Dong, Jingfu Liu*

State Key Laboratory of Environmental Chemistry and Ecotoxicology, Research Center for Eco-Environmental Sciences, Chinese Academy of Sciences, P.O. Box 2871, Beijing 100085, China

* Corresponding author.

Tel.: +86-10-62849192; Fax: +86-10-62849192

E-mail: jfliu@rcees.ac.cn

Environmental Science: Nano Accepted Manuscript

Abstract

Silver nanoparticles (AgNPs) are rather mutable in the water column, and the oxidation of AgNPs to release Ag^+ and reduction of Ag^+ to regenerate AgNPs existed simultaneously in certain compartments, making it rather difficult to monitor the reaction kinetics. In this study, we synthesized isotopically labeled AgNPs (99.5% ^{107}Ag, $^{107}AgNPs$) and $AgNO_3$ (99.81% ^{109}Ag, $^{109}AgNO_3$). For the first time, two Ag stable isotopes were used in the same experiment to track the transformation kinetics of AgNPs and Ag^+ in aquatic environments independently. It was found that the oxidation of AgNPs dominated the reaction in simple waters containing both $^{107}AgNPs$ and $^{109}Ag^+$. Sunlight significantly accelerated the dissolution of $^{107}AgNPs$, but longer solar irradiation (8 h) triggered aggregation of $^{107}AgNPs$ and therefore reduced the reaction rate. With the addition of 5 mg C/L dissolved organic matter, the reduction of $^{109}Ag^+$ played the leading role. The corrected concentration of dissolved $^{107}Ag^+$ began to decrease after some time, indicating other reduction mechanisms were happening. Elevated pH (pH 8.5) could even completely inhibit the oxidation of $^{107}AgNPs$. All the reactions seemed stalled at low temperature (6 °C) except the dissolution of $^{107}AgNPs$ under solar irradiation, suggesting the nonnegligible effect of sunlight. The presence of divalent cations induced agglomeration of $^{107}AgNPs$, but the reduction of $^{109}Ag^+$ was not significantly affected. These findings implied that the transformation between AgNPs and Ag^+ was rather complex and greatly depended on the external conditions. Given the fact that Ag^+ has been shown to be much more toxic than AgNPs, the speciation change may dramatically impact the final toxicity and bioavailability, which calls a strong request for assessing environmental risks of AgNPs under more realistic conditions.

Environmental Science: Nano Accepted Manuscript

1. Introduction

Due to their excellent optical, electrical, catalytical and antimicrobial properties, silver nanoparticles (AgNPs) can find applications in a body of industrial processes and medical fields. Their superior antibacterial ability also encourages their use as constituents in an increasing range of daily consumer goods.[1] However, during the production, usage and disposal of these products, AgNPs would be inevitably released into the natural system, which raises particular concerns over their complicated interactions with the biosphere and the adverse ecological effects.[2-5]

The physical state and chemical form of nanoparticles (NPs) should be specially considered as they greatly affect the final fate, transport and related toxicity of NPs within natural systems.[6] AgNPs are far from environmentally inert, and once released into water, multiple chemical and physical transformations are expected to occur, such as aggregation, oxidation, dissolution and sulfidation,[7] during which the initial oxidation is regarded to be of ultimate importance, partially because it is the first step for AgNPs to react with reduced sulfur and chloride.[8] More importantly, the oxidation of AgNPs to release Ag^+ can significantly alter the potential toxicity and bioavailability of Ag from AgNPs.[9-11] The dissolution of AgNPs is a cooperative oxidation process involving both dissolved oxygen and protons,[12] and peroxide intermediates were produced via the oxidation of AgNPs by oxygen.[13-15] Other properties of AgNPs such as the particle size, shape, and surface coating,[16-19] and the surrounding variables including the solution ionic strength, specific ligands, and natural organic matter (NOM) could also largely affect the behavior of AgNPs.[12] On the other hand, because of the modest redox potential of silver ($\varphi^{\theta}(Ag^+/Ag^0) = 0.80$ V), Ag^+ can also be reduced to AgNPs by some reducing agents in the environment, such as the omnipresent dissolved organic matter (DOM). A myriad of functional groups, including phenolic−OH, quinones, hydroxyls, and ketones, contained in DOM create a perfect reductive environment for the reduction of Ag^+, and

Environmental Science: Nano Accepted Manuscript

DOM related formation of AgNPs have been extensively reported. Humic acid (HA) and fulvic acid (FA) of different origins could drive the generation of AgNPs under environmentally relevant conditions, and the reduction kinetics of Ag^+ was enhanced considerably at elevated temperature and pH.[20, 21] Sunlight was reported to accelerate the reduction of Ag^+, and superoxide generated from solar irradiation of phenol groups in DOM was involved in the reduction.[22, 23] Moreover, the reconstitution of AgNPs from bulk objects was also observed under ambient conditions at relative humidity higher than 50%, revealing the mutable nature of AgNPs.[24, 25]

Our previous study demonstrated that AgNPs are highly dynamic in certain aquatic compartments, and the release of Ag^+ by oxidation of AgNPs and regeneration of AgNPs smaller than the primary NPs by reduction of Ag^+ could both occur in sunlit DOM-rich water.[26] Due to the different environmental behaviors of AgNPs and Ag^+ in the aquatic system and the distinct toxicity to particular organisms, speciation changes may significantly affect the final fate and bioeffects of AgNPs. However, as these two reverse processes occur simultaneously, it is difficult to monitor the reaction course, and rather large knowledge gaps exist, including the dominated process of the reactions, the reaction kinetics, and how environmental factors affecting the transformation. To overcome these gaps, several methods have been developed based on labeled NPs and ions, including labeling with radioisotopes, enriched stable isotopes and dyes/phase contrasting agents.[27] Among these labeling methods, stable isotope tracing is much more preferred for its easy handling and without the post-synthesis manipulation.[27-29] The stable isotope labeling method has been used to detect the toxicity and bioaccumulation of several types of NPs with high sensitivity and reliability.[27, 28, 30-34]

In this study, we synthesized isotopically labeled AgNPs (99.5% ^{107}Ag, $^{107}AgNPs$) and $AgNO_3$ (99.81% ^{109}Ag, $^{109}AgNO_3$). For the first time, two Ag stable isotopes were used in the same

Environmental Science: Nano Accepted Manuscript

experiment to track the transformation kinetics of AgNPs and Ag^+ in aquatic environments independently. The effects of several key environmental factors such as sunlight, DOM, solution pH, temperature, and divalent cations on the reaction kinetics were evaluated thoroughly, which would deepen our insight into the environmental behaviors of AgNPs.

2. Experimental

2.1 Materials

$AgNO_3$ (>99.5% purity) and ultrapure silver foil (>99.9% purity) were purchased from Sinopharm Chemical Reagent Co. Ltd. (Shanghai, China). ^{107}Ag and ^{109}Ag isotope (99+ % enriched) in solid form were purchased from Trace Sciences International Inc. (Pilot Point, TX). Trisodium citrate dihydrate (>99% purity), sodium borohydride (>99.99%, trace metals basis) and 2-(N-morpholino)ethanesulfonic acid (>99% purity) were purchased from Sigma Aldrich. High purity nitric acid was purchased from Merck (Darmstadt, Germany). Suwannee river humic acid (SRHA) was from the International Humic Substances Society (IHSS, St. Paul, MN). Ag^+ standard (1000 mg/L) used for ICP-MS determination was from National Institute of Metrology (Beijing, China). Other reagents were purchased from Beijing Chemicals with analytical purity or higher (Beijing, China). All the reagents were used as obtained without further purification. Ultrapure water (18.3 MΩ) produced with a Milli-Q Gradient system (Millipore, Billerica, MA) was used throughout the experiment.

2.2 Synthesis of the Isotopically Enriched AgNPs and Ag^+

Citrate-coated AgNPs (with natural isotope abundances) were synthesized following a previous method with slight modification.[29, 35] Briefly, 0.43 mL of 58.8 mmol/L $AgNO_3$ and 3.7 mL of 34 mmol/L trisodium citrate dihydrate were added into 100 mL of boiling distilled water, and then 1 mL of 50 mmol/L sodium borohydride was drop-wise added into the solution under vigorous stirring.

Environmental Science: Nano Accepted Manuscript

The solution turned from colorless to yellow immediately, and the color deepened with further addition of sodium borohydride. After stirring for another 30 min, the reaction vessel was taken out from the heating plate and allowed to cool to room temperature. The soluble byproducts were removed by centrifugal ultrafiltration (Amicon Ultra-15 100 kD, Millipore, MA), and AgNPs were further purified with ultrapure water three times, after which the stock suspension was stored at 4 ℃ in the dark for later use. For the synthesis of ^{107}AgNPs, the only difference was that ^{107}Ag isotope metal was first dissolved in HNO_3 and followed by evaporation to dryness to get the nitrate salt. $^{109}AgNO_3$ was also obtained by dissolving ^{109}Ag isotope metal in HNO_3. Silver foil with natural isotope abundances was used to optimize the synthesis parameter first.

2.3 Characterization of AgNPs

Transmission electron microscope (TEM) and energy dispersive X-ray spectroscopy (EDS) analysis were carried out with an H-7500 (Hitachi, Japan) at 80 kV or a high resolution TEM coupled with an EDS (TECNAI G20, FEI, Hillsboro OR) at 200 kV. TEM samples were prepared by placing 5 μL aliquots of the aqueous sample onto an ultrathin carbon-coated copper grid and drying in a vacuum drying oven. The UV-vis spectra from 250–800 nm were obtained by using a Shimadzu UV-3600 (Kyoto, Japan). The ζ potential and hydrodynamic diameter of AgNPs were characterized by dynamic light scattering (DLS) with a Zetasizer Nano (Malvern Instruments Ltd. Malvern, UK) at 25 ^{o}C. Specifically, stock AgNP suspensions were diluted with ultrapure water to a final concentration of 10 mg/L, and three measurements were performed to get the average value. The polydispersivity index (PDI), reported directly from the Zetasizer Nano ZS instrument when measuring the average hydrodynamic diameter, was also recorded to interpret the broadness of the size distribution.

2.4 Natural Organic Matter Solutions

Environmental Science: Nano Accepted Manuscript

SRHA was prepared at 1 g/L in ultrapure water and dissolved overnight on an end-over-end rotator at room temperature and then filtered through 0.45 μm membrane filters (mixed cellulose esters, Millipore, Billerica, MA). The dissolved organic carbon (DOC) was measured with a Phoenix 8000 total organic carbon analyzer (Tekmar-Dohrmann, Cincinnati, OH).

2.5 Silver Transformation Experiment

The experiments were conducted in a solar simulator (Beifanglihui CO., SN-500, Beijing) equipped with three 2500 W Xe lamps to simulate the sunlight. The irradiation intensity was maintained at 550 W/m^2, and bottles were immersed in a recirculating cooling water system to control the temperature. Three hundred milliliter suspensions containing 1 mg/L ^{107}AgNPs and 1 mg/L $^{109}Ag^+$ were prepared in 500 mL FEP (fluorinated ethylene propylene) bottles (Nalgene, Rochester, NY). In general experiments, pH was set to 7.4 and temperature was 30 °C. In each batch of the experiment, a dark control was performed in FEP bottles wrapped by three layers of aluminum foil and then one layer of black plastic bags and placed in the same simulator under similar conditions with the light-exposed ones. The effects of different parameters on the transformation of silver were evaluated. SRHA with a final concentration of 5 mg C/L was added in the system to investigate the effect of DOM. Silver transformation in the presence of SRHA at different pH values (5.6, 7.4 and 8.5) was also conducted. MES (2-(N-morpholino)ethanesulfonic acid) buffer (10 mM, pH 5.6) and borate buffers (1 mM, pH 7.4 and 8.5) were used for control of pH, and diluted HNO_3 and NaOH were used to adjust the pH values. Moreover, the effect of temperature (6, 30 and 50 °C) and divalent cations (40 mg/L Ca^{2+} and 24 mg/L Mg^{2+}) on the transformation kinetics of silver were also assessed. Stock solutions of $Ca(NO_3)_2$ and $Mg(NO_3)_2$ were prepared at concentrations of 40 and 24 g/L in ultrapure water. At each time interval during the experiment, 5 mL of the sample was taken from the bottle and mixed with 2.5 mL saturated EDTA solution for 10

Environmental Science: Nano Accepted Manuscript

min. Then the dissolved Ag was separated from AgNPs using ultrafiltration. The detailed separation method was shown in the following section 2.6. The filtrate was collected for further analysis after separation. Meanwhile, another 3 mL of the sample was taken to measure the UV-vis spectra. Three independent bottles were performed in each experiment.

2.6 Separation of AgNPs and Ag^+

In our previous study, the ultrafiltration method was proved to be an efficient approach to separate AgNPs and Ag^+, and the adsorption of Ag^+ on separation devices (Amicon Ultra-15 30 kD, Millipore, MA) was insignificant with recovery higher than 80%.[26] The same concentration of ^{107}AgNPs was used in this study, so the ultrafiltration method was also employed. It was reported that Ag^+ could easily adsorb onto AgNP surfaces, resulting in an obvious decrease in the free Ag^+.[12] The depletion of measured free Ag^+ in our case may cause the deviation of AgNP transformation kinetics. Therefore, EDTA, which was demonstrated to be able to efficiently eliminate the co-extraction of Ag^+ with AgNPs in previous studies,[36] was used as a complexing agent to reduce the adsorption of Ag^+ on surfaces of AgNPs in the experiment. To confirm that EDTA could not enhance the dissolution of AgNPs, suspensions containing 1 mg/L AgNPs and 100 mM EDTA (concentrations used in the experiment) were prepared and kept in the dark. At time intervals of 5 min, 10 min and 20 min, 5 mL of the samples were taken out to determine the dissolved Ag^+ concentration after ultrafiltration. No significant difference was observed. In our experiment, samples were mixed with EDTA for 10 min before ultrafiltration. Therefore, the effect of EDTA on the dissolution of AgNPs was negligible. By using the centrifugal ultrafilter tubes (30 kD), AgNPs as small as 2 nm could be retained in the upper filter devices.[26] We cannot exclude that some tiny AgNPs smaller than 2 nm may escape from the membrane, so in all cases in our study the dissolved Ag refers to all the dissolved Ag species that could pass through the filtration membranes, including

Environmental Science: Nano Accepted Manuscript

mainly free Ag^+, SRHA associated Ag^+, the adsorbed Ag^+ and any AgNPs < 2 nm.

2.7 Quantification and Calculation of Tracer Concentration

^{107}Ag and ^{109}Ag concentrations of the stock solutions ($^{107}AgNPs$ and $^{109}AgNO_3$) and the filtrates after separation were determined by Agilent 7700 ICP-MS (Santa Clara, CA, limit of detection of 0.009 μg/L), which was conducted with Ag standards, and the element In was used as the internal standard. For stock suspensions of $^{107}AgNPs$, HNO_3 digestion was performed before analysis. Briefly, 100 μL $^{107}AgNPs$ was mixed with 2 mL high purity HNO_3, and heated on a hot plate at 120 ^{o}C for 15 min. Then the solution was diluted for ICP-MS analysis. Blanks were conducted to control potential contaminations from reagents and containers, and silver contents in the blank samples were below the limit of detection of ICP-MS. After the experiment, the silver loss due to adsorption on the inner walls of bottles was also analyzed by decanting the solution and refilling the bottles with 1% HNO_3 followed by 4 h shaking to desorb the adsorbed silver.[37] Very limited silver (about 0.13% of the total silver content in the system) was detected by ICP-MS, showing silver losses to walls of 500 mL FEP bottles were insignificant.

An isotope tracing technique was employed to track two tracers, ^{107}Ag and ^{109}Ag, as described by Croteau et al.[33] Since the concentration of silver in reagents and container blanks was below the limit of detection of ICP-MS, we assume that silver present in the system was only from the two isotopes we added. Though the enrichment of two isotopes was not 100% (99.5% for ^{107}Ag and 99.81% for ^{109}Ag), the effect of ultratrace impurities on the final data was very limited. Therefore, we also assume that 100% ^{107}Ag was from ^{107}Ag enriched source and likewise for ^{109}Ag. The relative abundances of ^{107}Ag tracer (p^{107}) and ^{109}Ag tracer (p^{109}) in the calibration standards are also determined using the signal intensities of each Ag isotope (eq 1 and eq 2).[30, 33] p^{107} averaged 0.5150 $\pm$0.0037 (standard deviation) and p^{109} averaged 0.4850 $\pm$0.0037 for batches of samples analyzed on

Environmental Science: Nano Accepted Manuscript

different days，which were in agreement with the natural relative abundances of ^{107}Ag (0.5184) and ^{109}Ag (0.4816),[29] showing the obtained data were convincing.

$$p^{107} = \text{intensity}\left(\frac{^{107}\text{Ag}}{^{107}\text{Ag}+^{109}\text{Ag}}\right) \quad (1)$$

$$p^{109} = \text{intensity}\left(\frac{^{109}\text{Ag}}{^{107}\text{Ag}+^{109}\text{Ag}}\right) \quad (2)$$

Concentrations of tracer ^{107}Ag in the filtrate ([^{107}Ag]) are calculated as the product of p^{107} and the total Ag concentrations inferred by the ICP-MS software from the tracer intensity ([T^{107}Ag]), and concentrations of tracer ^{109}Ag in the filtrate ([^{109}Ag]) are calculated as the product of p^{109} and the total Ag concentrations inferred by the ICP-MS software from the tracer intensity ([T^{109}Ag]):

$$\left[^{107}\text{Ag}\right] = p^{107}\left[\text{T}^{107}\text{Ag}\right] \quad (3)$$

$$\left[^{109}\text{Ag}\right] = p^{109}\left[\text{T}^{109}\text{Ag}\right] \quad (4)$$

3. Results and Discussion

3.1 Characterization and Stability of AgNPs. As shown in Figure S1, the synthesized citrate-coated ^{107}AgNPs in this study are almost spherical with a mean size of 15.6 ± 4.3 nm by manual counting more than 200 individual particles. ^{107}AgNPs carried stable negative charges with ζ potential of -23.1 mV in ultrapure water, and in situ DLS gave a hydrodynamic diameter of 24.7 nm, larger than the TEM result due to the citrate coating, with a PDI of 0.378. Compared with previous literature[29] using the same method for the synthesis of ^{107}Ag labeled NPs, comparable particle size, shape and size distribution we can get, proving this method is quite repeatable. Though the enriched stable isotopes are expensive, this synthesis method provides a high yield (an average yield of 78%) and only needs several mg in a single synthesis,[29] which is affordable. During storage, a portion of the stock suspension was taken out for DLS analysis every month and results showed that no significant difference of the hydrodynamic diameter and ζ potential was observed during three months, revealing the ^{107}AgNP suspension was rather stable. In the experiment, the stock suspension

Environmental Science: Nano Accepted Manuscript

was kept no more than three months.

3.2 Effect of Light Irradiation. Diluted ^{107}AgNPs (1 mg/L) and $^{109}Ag^+$ solution (1 mg/L) were mixed together, and subjected to solar irradiation or kept in the dark to evaluate simulated sunlight on the transformation of AgNPs and Ag^+. As AgNPs are highly dynamic, the oxidation of AgNPs to release Ag^+ is expected to take place in the suspension.[12, 26] Moreover, the reduction of Ag^+ to Ag^0 by some capping agents was also reported in early studies.[38] Therefore, we monitored the time-resolved concentration of dissolved $^{107}Ag^+$ and $^{109}Ag^+$ during the experiment first. As shown in Figure 1A, the amount of dissolved $^{109}Ag^+$ only fluctuated on a very small scale both in the light and dark, and did not change much through the whole time, indicating that the reduction of Ag^+ in simple AgNP suspensions was not evident without additional reducing agents even under the solar irradiation. On the contrary, the concentration of dissolved $^{107}Ag^+$ increased rapidly in both cases, implying the fast oxidation of ^{107}AgNPs. It is noteworthy that the initial concentration of $^{107}Ag^+$ was not zero, and about 100 μg/L $^{107}Ag^+$ was detected in the system. The inevitable exposure to oxygen during dilution of stock suspensions may lead to the oxidation of AgNPs.[16] Furthermore, as the complexing agent EDTA was added during the separation procedure, the high concentration of $^{107}Ag^+$ may also ascribe to the adsorbed $^{107}Ag^+$ on surfaces of ^{107}AgNPs, because 50.6 μg/L $^{107}Ag^+$ was measured without EDTA. A previous study also reported that the addition of 2 mg/L AgNPs into 0.3 mg/L Ag^+ solution led to a rapid decrease (about 100 μg/L) in dissolved Ag^+ concentration.

According to previous studies, the oxidation reaction of AgNPs can be written as eq (5):[12]

$$Ag_{(s)} + \frac{1}{2}O_{2(aq)} + 2H^+_{(aq)} \leftrightarrow 2Ag^+_{(aq)} + H_2O_{(l)} \quad (5)$$

The concentration of H^+ and dissolved O_2 are supposed to be constant over time, so the oxidation of ^{107}AgNPs followed a pseudo first-order rate law:[16]

$$[^{107}Ag^+]_t = [^{107}Ag^0]_0[1 - \exp(-kt)] \quad (6)$$

Environmental Science: Nano Accepted Manuscript

in which $[^{107}Ag^{+}]_t$ is the released concentration of $^{107}Ag^{+}$ at time *t*, $[^{107}Ag^{0}]_0$ is the concentration of ^{107}AgNPs at the beginning of the experiment, *k* is the rate constant, and *t* is the reaction time. Taking logarithm of eq (6), we can get the following equation:

$$\ln\left(\frac{[^{107}Ag^{0}]_0-[^{107}Ag^{+}]_t}{[^{107}Ag^{0}]_0}\right) = -kt \quad (7)$$

We assume that 100% ^{107}Ag was from ^{107}Ag enriched source, so $[^{107}Ag^{0}]_t$, the concentration of ^{107}AgNPs at time *t*, can be obtained by the difference of the concentration of ^{107}AgNPs at initial time ($[^{107}Ag^{0}]_0$) and the released concentration of $^{107}Ag^{+}$ at time *t* ($[^{107}Ag^{+}]_t$). Thus, eq (7) can be written as:

$$\ln\left(\frac{[^{107}Ag^{0}]_t}{[^{107}Ag^{0}]_0}\right) = -kt \quad (8)$$

The curve obtained by plotting $\ln\left(\frac{[^{107}Ag^{0}]_t}{[^{107}Ag^{0}]_0}\right)$ *versus* time for ^{107}AgNPs (Figure 1B) in the dark is linear with R^2 = 0.9787, indicating that the ion release of $^{107}Ag^{+}$ obeyed the first-order kinetics well. However, the fitting line was divided into two stages in the light. During the first 12 h, the oxidation of ^{107}AgNPs was much more rapid with the dissolution rate constant of 0.0366 h^{-1}, about 4 times higher than that in the dark. Light induced fast dissolution of AgNPs was also observed in other studies,[26] and photoaging that the gradual formation of an oxide shell around metallic silver cores under light irradiation may shed some light on the phenomenon.[39] After 12 h, the release rate of $^{107}Ag^{+}$ slowed down. Considering that solar irradiation could degrade the capping agents of AgNPs like citrate and PVP, which may induce the aggregation of AgNPs,[26, 37, 40-42] we speculate that the decreased oxidation rate was ascribed to the coarsening of ^{107}AgNPs. A previous study also reported that loss of accessibility of reactive sites due to the aggregation process decreased the dissolution rate constant of AgNPs.[43] To this end, UV-vis spectra of AgNPs at different time intervals were measured (Figure S2). The SPR peak position in the dark did not alter dramatically except a decrease in the absorption with time and a little blue shift of λ_{max}, implying that ^{107}AgNPs in the dark

Environmental Science: Nano Accepted Manuscript

were rather stable without agglomeration. For ^{107}AgNPs under solar irradiation, no significant change in the SPR peak shape was observed during the first 8 h; however, obvious broadening of the peak width occurred after that, indicating the aggregation of ^{107}AgNPs. Meanwhile, we monitored the morphology change of AgNPs by TEM. Figure 1C and 1D demonstrated that ^{107}AgNPs in the dark were well dispersed even after 2 days' reaction. However, light-triggered shape transformation was observed for ^{107}AgNPs exposed to simulated sunlight. In accord with the UV-vis spectra results, ^{107}AgNPs were stable in the first several hours (Figure S2C). However, with longer solar irradiation, adjacent particles tended to fuse together to form larger particles and worm-like structures (Figure 1E), which explained the SPR peak broadening in the UV-vis spectra. As time went on, more particles were involved to form large aggregates (Figure 1F), causing significant decrease of ^{107}AgNPs surface areas, which may contribute to the retarded release rate of $^{107}Ag^+$ in the light.

3.3 Effect of Dissolved Organic Matter. Our earlier study reported that the oxidation of AgNPs to release Ag^+ and the reduction of Ag^+ to form new AgNPs by DOM could both happen in sunlit DOM-rich water, which considerably affected the fate and transport of AgNPs in the environment.[26] In order to gain important information on these two reverse processes, SRHA, used as a model HA, was added in the mixture of ^{107}AgNPs and $^{109}Ag^+$ to evaluate the reaction kinetics. The real-time contents of dissolved Ag^+ in the light and dark were both recorded. The concentration of dissolved $^{109}Ag^+$ decreased dramatically in both cases, revealing the fast reduction of Ag^+ by SRHA. According to previous studies, the reduction of Ag^+ by DOM obeyed the pseudo-first-order reaction,[23] that is:

$$\frac{\mathrm{d}[^{109}\mathrm{AgNP}]}{\mathrm{d}t} = k[^{109}\mathrm{Ag}^+]_t \quad (9)$$

where d[^{109}AgNP] is the concentration change of ^{109}AgNPs in short period of time dt, [$^{109}Ag^+$]$_t$ is the concentration of $^{109}Ag^+$ at time t, and k is the rate constant.

Environmental Science: Nano Accepted Manuscript

Here we assume that all the $^{109}Ag^{+}$ reduced was transformed into ^{109}AgNPs in the presence of SRHA, so [^{109}AgNP] can be obtained by the difference of the concentration of $^{109}Ag^{+}$ at initial time ($[^{109}Ag^{+}]_0$) and at time *t* ($[^{109}Ag^{+}]_t$). After the integral of the equation, eq (9) can be written as:

$$[^{109}Ag^{+}]_t = [^{109}Ag^{+}]_0 \exp(-kt) \quad (10)$$

Taking logarithm of eq (10), we can get the following equation:

$$\ln\left(\frac{[^{109}Ag^{+}]_t}{[^{109}Ag^{+}]_0}\right) = -kt \quad (11)$$

Eq (11) fitted well to the data of dissolved $^{109}Ag^{+}$ (Figure 2A), and the reduction rate constant under solar irradiation (0.0051 h^{-1}) was approximately 2 times larger than that in the dark (0.0017 h^{-1}), revealing that sunlight greatly promoted the regeneration of AgNPs.[22, 23] Additionally, we also took TEM images to confirm the formation of new AgNPs. As shown in Figure 2C and S3, a large number of smaller NPs in the size range of 2-6 nm were appeared around the original AgNPs (about 15 nm) both in the light and dark after 24 h's experiment. Higher resolution TEM images (Figure 2D and S3B) demonstrated that the lattice fringe spacing of these small NPs was about 2.4 Å, corresponding to the (111) lattice plane of the face-centered cubic structure of metallic silver. Moreover, EDS data (Figure 2E and S3C) also represented high signals of Ag, proving the small particles were AgNPs. The strong signals of Cu and C were mostly attributed to the carbon supported copper grid. As original ^{107}AgNPs have a narrow size distribution, and the release of $^{107}Ag^{+}$ was not high (Figure 2B, only about 17% silver was in ionic form), we can exclude the possibility that the dissolution of pristine ^{107}AgNPs (15 nm) gave rise to the formation of small AgNPs (2-6 nm).

Since the recrystallization of AgNPs from Ag^{+} could not be ignored, the measured data of dissolved $^{107}Ag^{+}$ was corrected based on the fitted reduction equation given in Figure 2A, and the corrected ion release kinetics of ^{107}AgNPs was shown in Figure 2B. The concentration of dissolved

Environmental Science: Nano Accepted Manuscript

$^{107}Ag^{+}$ gradually increased due to the oxidation of ^{107}AgNPs. However, after about 12 h, the curve dropped sharply for both in the light and dark. The maximum concentration of dissolved $^{107}Ag^{+}$ was much lower than that without SRHA as well. The inhibited ion release of AgNPs in the presence of DOM was extensively reported elsewhere, and was ascribed to either the blocking of oxidation sites of AgNPs by the adsorption of DOM, or the reduced amount of peroxide intermediates owing to their competitive reaction with DOM.[12, 26] As the amount of dissolved $^{107}Ag^{+}$ reconstituted to ^{107}AgNPs had been compensated by the fitted reduction equation, the unusual decrease of dissolved $^{107}Ag^{+}$ indicated that there might be other pathways that contributed to the $^{107}Ag^{+}$ reduction. For example, previous studies have reported that AgNPs could serve as catalysts to facilitate the reduction of Ag^{+} on their surfaces, which resulted in a rapid AgNP growth stage.[20, 44-47] In our study, the initial concentration of $^{109}Ag^{+}$ in the solution was relatively high, and the coating of SRHA on AgNPs also provided a physical barrier that made it harder for the released $^{107}Ag^{+}$ to diffuse into the bulk solution. As a result, most of $^{107}Ag^{+}$ might adsorb on the surface of ^{107}AgNPs or stay around ^{107}AgNP cores, which promoted the autocatalysis by ^{107}AgNPs. However, as the oxidation of ^{107}AgNPs happened at the same time, it was impossible to trace the autocatalysis process. Compared with the rapid reduction of $^{109}Ag^{+}$, the oxidation of ^{107}AgNPs is very limited. Therefore, the dissolution of formed ^{109}AgNPs should be unremarkable in our study.

3.4 Effect of pH. pH is an important parameter that may influence the thermodynamic equilibrium of AgNPs,[12] thus the reaction kinetics of ^{107}AgNPs and $^{109}Ag^{+}$ at different pH values was evaluated in this study. In the tested pH range (5.6 − 8.5), there is an obvious decrease in the concentration of $^{109}Ag^{+}$ during the experiment. By fitting the collected data to eq (11), linear lines were obtained. The reaction rate coefficient elevated (the slope of lines became more negative) with increasing solution pH. As shown in Figure 3, the reaction rate constant under solar irradiation

Environmental Science: Nano Accepted Manuscript

increased about 4 times from 0.0025 h^{-1} at pH 5.6 to 0.0098 h^{-1} at pH 8.5, which also happened for the dark counterpart, though the reaction rate coefficient was much lower. pH-dependent reduction of Ag^+ was also reported in prior studies.[22, 23] It was demonstrated that there existed a linear relationship between the redox potential of HA solution and pH, and the much lower redox potential of HA at higher pH accelerated the reduction of Ag^+.[22] Ligand-to-metal charge transfer pathway was also reported to be involved in the reduction of Ag^+, in which Ag^+ first bound with HA and electron transferred between Ag^+ and HA induced the AgNP generation. At high pH, HA was more negative and strong electrostatic attraction between positively charged Ag^+ and negatively charged HA enhanced the complexing of HA with Ag^+, thus promoted the Ag^+ reduction.[23]

The concentration of dissolved $^{107}Ag^+$ showed a similar trend at pH 5.6 with that at pH 7.4 after correction, which first increased for some time and then decreased gradually, suggesting that the autocatalysis process may occur as well. As oxygen and proton both participated in the oxidation of AgNPs,[12] lower pH facilitated the dissolution of AgNPs, which explained the higher concentration of dissolved $^{107}Ag^+$ at pH 5.6. However, the dissolution behavior of AgNPs at pH 8.5 was different. The measured $^{107}Ag^+$ concentration dropped from the initial of the reaction. As $^{107}Ag^+$ could also be reduced by DOM, we can get a similar equation with eq (11):

$$\ln\left(\frac{[^{107}Ag^+]_t}{[^{107}Ag^+]_0}\right) = -kt \qquad (12)$$

The measured $^{107}Ag^+$ concentration fitted well with eq (12). Furthermore, the reaction rate coefficients were almost equal to that of the reduction of dissolved $^{109}Ag^+$ under the same conditions (0.0051 h^{-1} for $^{109}Ag^+$ *vs* 0.0052 h^{-1} for $^{107}Ag^+$ in the dark and 0.0098 h^{-1} for $^{109}Ag^+$ *vs* 0.010 h^{-1} for $^{107}Ag^+$ in the light), which indicated that the oxidation of ^{107}AgNPs was negligible. Compared with our previous study,[26] though the dissolution of AgNPs was not favored at high pH, the release of Ag^+ was still detectable in AgNP suspensions at pH 8.3 under similar conditions. The varied behavior of

Environmental Science: Nano Accepted Manuscript

AgNPs implied that the pre-addition of Ag^+ in the system affected the Ag^0/Ag^+ coexistence equilibrium of AgNPs, which may subsequently influence the final fate and transformation of AgNPs.

3.5 Effect of Temperature. The influence of temperature on the reaction kinetics was also evaluated. Results (Figure S4A) showed that an increase of temperature accelerated the reduction of $^{109}Ag^+$, resulting in larger reaction rate constants both in the light and dark. However, higher temperature had little influence on the dissolution of $^{107}Ag^+$ (Figure S4B), probably because the presence of large numbers of dissolved $^{109}Ag^+$ in the solution inhibited further oxidation of ^{107}AgNPs. At low temperature, the reduction of $^{109}Ag^+$ was significantly retarded both in the light and dark, and the concentration of dissolved $^{109}Ag^+$ almost remained constant during the whole time (Figure S4C), which was also the case for the oxidation of ^{107}AgNPs in the dark. However, the concentration of dissolved $^{107}Ag^+$ progressively increased under solar exposure even at 6 ^{o}C (Figure S4D). Heat generation by metal NPs under optical illumination has been extensively studied[48-50] and previous researches have reported that the surface temperature of metal NPs could reach well above the boiling point of water under proper illumination.[50] The oxidation of ^{107}AgNPs at low temperature was mostly due to the photothermal effect of AgNPs, which emphasized that solar irradiation was a vital factor that cannot be ignored in assessing the environmental behavior of AgNPs.

3.6 Effect of Ca^{2+} and Mg^{2+}. Divalent metal ions like Ca^{2+} and Mg^{2+} are ubiquitous in natural waters, and they can largely affect the stability and transport of NPs.[37, 51] $Ca(NO_3)_2$ and $Mg(NO_3)_2$ under environmentally relevant concentrations were added in the system to assess their influence on the reaction kinetics. The solution turned from yellow to dark red up on spiking of $Ca(NO_3)_2$ and $Mg(NO_3)_2$. Meanwhile, time-dependent UV-vis spectra (Figure 4) also demonstrated that a tailing peak appeared following the main SPR peak, suggesting that divalent metal ions triggered the

Environmental Science: Nano Accepted Manuscript

aggregation of AgNPs. For samples kept in the dark, the characteristic SPR absorption did not change much over time, while the absorption of the tail peak gradually grew with longer light irradiation, indicating further agglomeration of AgNPs, which again proved the significant effect of light on the transformation of AgNPs. The related shape transformation of AgNPs was confirmed by the following TEM images. From Figure 4E, it was clearly observed the bridging of neighboring AgNPs after the addition of divalent metal ions. Compared with the presence of small coagulations in the dark after the experiment, particles exposed to light appeared to be relatively more agglomerated. Much more initial AgNPs and regenerated tiny particles were participated in the growing of large aggregates, resulting in amorphous, unshaped structures.

Though AgNPs aggregated in the presence of divalent metal ions, the reduction of $^{109}Ag^{+}$ was not strongly affected, as the variation of fitted reaction rate coefficients was very limited (0.0017 h^{-1} with divalent ions *vs* 0.0017 h^{-1} without divalent ions in the dark, and 0.0048 h^{-1} with divalent ions *vs* 0.0051 h^{-1} without divalent ions in the light). It was likely due to the reduction of $^{109}Ag^{+}$ taking place in homogeneous solutions which were not greatly influenced by the shape shift of ^{107}AgNPs. As for the release of $^{107}Ag^{+}$, since the aggregation of ^{107}AgNPs considerably reduced effective surface areas, the oxidation of ^{107}AgNPs was hindered in the dark, resulting in a negligible change of the concentration of dissolved $^{107}Ag^{+}$. However, because of the photothermal effect of light, an evident increase of dissolved $^{107}Ag^{+}$ was still measured. The decline of surface areas of ^{107}AgNPs may restrict the autocatalysis reaction on the surface of ^{107}AgNPs, thus the subsequent decrease of dissolved $^{107}Ag^{+}$ became much slower.

To compare the influence of individual environmental factors on the transformation kinetic of AgNPs and Ag^{+} in aquatic systems, all the reaction kinetic constants were summarized in Table S1 and S2 of the Supporting Information.

Environmental Science: Nano Accepted Manuscript

4. Conclusions

Our previous study[26] has shown that inevitable environmentally relevant factors such as sunlight and DOM can influence the transformation of AgNPs in aquatic systems. The cycle of chemical oxidation of AgNPs to release Ag^+ and regeneration to form AgNPs exists in sunlit DOM-rich water. However, as the two reverse processes occur simultaneously, it is difficult to monitor the reaction course, which leaves a large knowledge gap, such as the dominated process of the reactions, the reaction kinetics, and how environmental factors affect the transformation kinetics. In this work, the double stable isotope labeling method (stable isotope labeled ^{107}AgNPs and $^{109}AgNO_3$ mixed in the same experiment) was used to investigate the speciation variation of silver in the water column, and much more information on the transformation kinetics of silver was obtained. In pure water containing both ^{107}AgNPs and $^{109}Ag^+$, the oxidation of ^{107}AgNPs dominated the reaction, resulting in a substantial content of total dissolved Ag^+. Sunlight played dual functions in the process. On the one hand, solar exposure greatly accelerated the oxidation of ^{107}AgNPs, and a much higher initial reaction rate constant was obtained than that in the dark (0.0366 h^{-1} *vs* 0.0078 h^{-1}). On the other hand, light irradiation induced the aggregation of ^{107}AgNPs, causing the release of dissolved $^{107}Ag^+$ to slow down with time. However, the reduction of $^{109}Ag^+$ played the leading role in the presence of DOM, especially for samples under solar irradiation. The reaction rate coefficient was almost two times larger than the counterparts in the dark. DOM suppressed the oxidation of ^{107}AgNPs, and only a small portion of dissolved $^{107}Ag^+$ was detected. Additionally, other reduction mechanisms might happen on the surface of ^{107}AgNPs, causing the concentration of dissolved $^{107}Ag^+$ to decrease after some time. As Ag^+ has been shown to be much more toxic than AgNPs,[10, 11, 52] the reduction of dissolved Ag^+ in DOM-rich water suggests that the overall toxicity might be mitigated to some extent. Meanwhile, the enhanced stabilizing effect of DOM could disperse AgNPs in aquatic

Environmental Science: Nano Accepted Manuscript

systems for a long time, which means that AgNPs may act as a reservoir of Ag^+ to cause persistent adverse effects. Furthermore, in areas where the use of AgNPs was not wide, there could still be some level of AgNPs due to the possible transport of AgNPs from the point of origin. At relatively low temperatures, though other reactions seemed lagged, the concentration of dissolved $^{107}Ag^+$ still increased gradually under solar irradiation, indicating the photothermal effects cannot be neglected. The spiking of divalent cations triggered agglomeration of ^{107}AgNPs, but the reformation rate of ^{109}AgNPs was not largely affected. According to previous studies,[22] newly formed AgNPs were also prone to form large aggregates or even settled down in the presence of Ca^{2+} and Mg^{2+}. The decline in dissolved Ag^+ and coarsening of AgNPs may also alleviate AgNPs' threat to aquatic organisms to a certain degree. It is reported that the estimated concentration of AgNPs in the river was in the range of 30−320 ng/L in the maximum scenarios,[53] which is much lower than that we used in our experiment. To better understanding the fate of AgNPs in natural environments, further research exploring the transformation of AgNPs under more realistic conditions is needed.

Acknowledgements

This work was supported by the National Natural Science Foundation of China (21507147, 21337004, 21227012), and the Strategic Priority Research Program of the Chinese Academy of Sciences (XDB14020101).

Supporting Information

Additional results are provided in Supporting Information.

References

1. S. J. Yu, Y. G. Yin and J. F. Liu, *Environ. Sci.: Processes Impacts*, 2013, **15**, 78-92.
2. M. E. Quadros and L. C. Marr, *Environ. Sci. Technol.*, 2011, **45**, 10713-10719.
3. M. E. Quadros, R. Pierson, N. S. Tulve, R. Willis, K. Rogers, T. A. Thomas and L. C. Marr, *Environ. Sci. Technol.*, 2013, **47**, 8894-8901.
4. D. Cleveland, S. E. Long, P. L. Pennington, E. Cooper, M. H. Fulton, G. I. Scott, T. Brewer, J. Davis, E. J. Petersen and L. Wood, *Sci. Total Environ.*, 2012, **421**, 267-272.
5. L. Geranio, M. Heuberger and B. Nowack, *Environ. Sci. Technol.*, 2009, **43**, 8113-8118.

Environmental Science: Nano Accepted Manuscript

6. G. V. Lowry, K. B. Gregory, S. C. Apte and J. R. Lead, *Environ. Sci. Technol.*, 2012, **46**, 6893-6899.
7. C. Levard, E. M. Hotze, G. V. Lowry and G. E. Brown, *Environ. Sci. Technol.*, 2012, **46**, 6900-6914.
8. C. Levard, S. Mitra, T. Yang, A. D. Jew, A. R. Badireddy, G. V. Lowry and G. E. Brown, Jr., *Environ. Sci. Technol.*, 2013, **47**, 5738-5745.
9. C. N. Lok, C. M. Ho, R. Chen, Q. Y. He, W. Y. Yu, H. Sun, P. K. H. Tam, J. F. Chiu and C. M. Che, *J. Biol. Inorg.Chem.*, 2007, **12**, 527-534.
10. Z. Xiu, Q. Zhang, H. L. Puppala, V. L. Colvin and P. J. J. Alvarez, *Nano lett.*, 2012, **12**, 4271-4275.
11. Z. M. Xiu, J. Ma and P. J. J. Alvarez, *Environ. Sci. Technol.*, 2011, **45**, 9003-9008.
12. J. Y. Liu and R. H. Hurt, *Environ. Sci. Technol.*, 2010, **44**, 2169-2175.
13. D. He, S. Garg and T. D. Waite, *Langmuir*, 2012, **28**, 10266-10275.
14. D. He, A. M. Jones, S. Garg, A. N. Pham and T. D. Waite, *J. Phys. Chem. C*, 2011, **115**, 5461-5468.
15. A. M. Jones, S. Garg, D. He, A. N. Pham and T. D. Waite, *Environ. Sci. Technol.*, 2011, **45**, 1428-1434.
16. W. Zhang, Y. Yao, N. Sullivan and Y. S. Chen, *Environ. Sci. Technol.*, 2011, **45**, 4422-4428.
17. R. Ma, C. Levard, S. M. Marinakos, Y. W. Cheng, J. Liu, F. M. Michel, G. E. Brown and G. V. Lowry, *Environ. Sci. Technol.*, 2012, **46**, 752-759.
18. J. Y. Liu, D. A. Sonshine, S. Shervani and R. H. Hurt, *ACS Nano*, 2010, **4**, 6903-6913.
19. Y. Li, W. Zhang, J. Niu and Y. Chen, *Environ. Sci. Technol.*, 2013, **47**, 10293-10301.
20. N. F. Adegboyega, V. K. Sharma, K. Siskova, R. Zboril, M. Sohn, B. J. Schultz and S. Banerjee, *Environ. Sci. Technol.*, 2013, **47**, 757-764.
21. N. Akaighe, R. I. MacCuspie, D. A. Navarro, D. S. Aga, S. Banerjee, M. Sohn and V. K. Sharma, *Environ. Sci. Technol.*, 2011, **45**, 3895-3901.
22. Y. G. Yin, J. F. Liu and G. B. Jiang, *ACS Nano*, 2012, **6**, 7910–7919.
23. W. C. Hou, B. Stuart, R. Howes and R. G. Zepp, *Environ. Sci. Technol.*, 2013, **47**, 7713-7721.
24. R. D. Glover, J. M. Miller and J. E. Hutchison, *ACS Nano*, 2011, **5**, 8950-8957.
25. M. R. Wiesner, G. V. Lowry, E. Casman, P. M. Bertsch, C. W. Matson, R. T. Di Giulio, J. Liu and M. F. Hochella, Jr., *ACS Nano*, 2011, **5**, 8466-8470.
26. S. J. Yu, Y. G. Yin, J. B. Chao, M. H. Shen and J. F. Liu, *Environ. Sci. Technol.*, 2014, **48**, 403-411.
27. S. K. Misra, A. Dybowska, D. Berhanu, M. N. Croteau, S. N. Luoma, A. R. Boccaccini and E. Valsami-Jones, *Environ. Sci. Technol.*, 2012, **46**, 1216-1222.
28. A. D. Dybowska, M.-N. Croteau, S. K. Misra, D. Berhanu, S. N. Luoma, P. Christian, P. O'Brien and E. Valsami-Jones, *Environ. Pollut.*, 2011, **159**, 266-273.
29. A. Laycock, B. Stolpe, I. Roemer, A. Dybowska, E. Valsami-Jones, J. R. Lead and M. Rehkamper, *Environ. Sci.: Nano*, 2014, **1**, 271-283.
30. M. N. Croteau, D. J. Cain and C. C. Fuller, *Environ. Sci. Technol.*, 2013, **47**, 3424-3431.
31. A. Bourgeault, C. Cousin, V. Geertsen, C. Cassier-Chauvat, F. Chauvat, O. Durupthy, C. Chaneac and O. Spalla, *Environ. Sci. Technol.*, 2015, **49**, 2451-2459.
32. F. Larner and M. Rehkaemper, *Environ. Sci. Technol.*, 2012, **46**, 4149-4158.
33. M. N. Croteau, A. D. Dybowska, S. N. Luoma, S. K. Misra and E. Valsami-Jones, *Environ. Chem.*, 2014, **11**, 247-256.
34. A. Laycock, M. Diez-Ortiz, F. Larner, A. Dybowska, D. Spurgeon, E. Valsami-Jones, M. Rehkamper and C. Svendsen, *Environ. Sci. Technol.*, 2016, **50**, 412-419.
35. J. Gigault and V. A. Hackley, *Anal. Chim. Acta*, 2013, **763**, 57-66.
36. G. Hartmann, C. Hutterer and M. Schuster, *J. Anal. At. Spectrom.*, 2013, **28**, 567-572.
37. X. Li and J. J. Lenhart, *Environ. Sci. Technol.*, 2012, **46**, 5378-5386.
38. C. E. Hoppe, M. Lazzari, I. Pardinas-Blanco and M. A. Lopez-Quintela, *Langmuir*, 2006, **22**, 7027-7034.
39. N. Grillet, D. Manchon, E. Cottancin, F. Bertorelle, C. Bonnet, M. Broyer, J. Lerme and M. Pellarin, *Journal of Physical Chemistry C*, 2013, **117**, 2274-2282.

Environmental Science: Nano Accepted Manuscript

40. Y. W. Cheng, L. Y. Yin, S. H. Lin, M. Wiesner, E. Bernhardt and J. Liu, *J. Phys. Chem. C*, 2011, **115**, 4425-4432.
41. C. Xue, G. S. Metraux, J. E. Millstone and C. A. Mirkin, *J. Am. Chem. Soc.*, 2008, **130**, 8337-8344.
42. Y. Li, J. F. Niu, E. X. Shang and J. Crittenden, *Environ. Sci. Technol.*, 2014, **48**, 4946-4953.
43. D. He, M. W. Bligh and T. D. Waite, *Environ. Sci. Technol.*, 2013, **47**, 9148-9156.
44. Z. Zaheer and Rafiuddin, *Int. J. Chem. Kinet.*, 2012, **44**, 680-691.
45. X. H. Li, H. B. Li, G. D. Li and J. S. Chen, *Inorg. Chem.*, 2009, **48**, 3132-3138.
46. A. Kytsya, L. Bazylyak, Y. Hrynda, A. Horechyy and Y. Medvedevdkikh, *Int. J. Chem. Kinet.*, 2015, **47**, 351-360.
47. R. Patakfalvi, S. Papp and I. Dekany, *J. Nanopart. Res.*, 2007, **9**, 353-364.
48. A. O. Govorov and H. H. Richardson, *Nano Today*, 2007, **2**, 30-38.
49. H. H. Richardson, Z. N. Hickman, A. O. Govorov, A. C. Thomas, W. Zhang and M. E. Kordesch, *Nano Lett.*, 2006, **6**, 783-788.
50. O. Neumann, A. S. Urban, J. Day, S. Lal, P. Nordlander and N. J. Halas, *ACS Nano*, 2013, **7**, 42-49.
51. X. Li, J. J. Lenhari and H. W. Walker, *Langmuir*, 2012, **28**, 1095-1104.
52. M. H. Shen, X. X. Zhou, X. Y. Yang, J. B. Chao, R. Liu and J. F. Liu, *Sci. Rep.*, 2015, **5**, 9674.
53. S. A. Blaser, M. Scheringer, M. MacLeod and K. Hungerbuhler, *Sci. Total Environ.*, 2008, **390**, 396-409.

Environmental Science: Nano Accepted Manuscript

Figure Captions

Figure 1. Transformation of AgNPs and Ag^+ in pure water. Change of dissolved $^{109}Ag^+$ over time (A); Fraction of metallic ^{107}AgNPs over time (B); and TEM images of AgNPs in the dark after 0 h (C) and 48 h (D), and in the light after 8 h (E) and 48 h (F). A mixture of 1 mg/L ^{107}AgNPs and 1 mg/L $^{109}Ag^+$ in pure water was treated at pH 7.4 and 30 °C.

Figure 2. Transformation of AgNPs and Ag^+ in the presence of SRHA. Fraction of dissolved $^{109}Ag^+$ over time (A); Ion release kinetics of ^{107}AgNPs over time (B); and TEM image of AgNPs in the light after 24 h (C), and the HRTEM image (D) and EDS analysis (E) of the new AgNPs. A mixture of 1 mg/L ^{107}AgNPs, 1 mg/L $^{109}Ag^+$ and 5 mg C/L SRHA was treated at pH 7.4 and 30 °C.

Figure 3. Fraction of dissolved $^{109}Ag^+$ and ion release kinetics of ^{107}AgNPs over time at different pH values. Fraction of dissolved $^{109}Ag^+$ at pH 5.6 and 8.5 (A), ion release kinetics of ^{107}AgNPs at pH 5.6 (B), Fraction of dissolved $^{107}Ag^+$ at pH 8.5 (C). A mixture of 1 mg/L ^{107}AgNPs, 1 mg/L $^{109}Ag^+$, and 5 mg C/L SRHA was treated at 30 °C.

Figure 4. Impact of divalent cations on the transformation of AgNPs and Ag^+. UV−vis absorption spectra of AgNPs: in the light (A) and dark (B); Fraction of dissolved $^{109}Ag^+$ (C) and ion release kinetics of ^{107}AgNPs (D) over time; and TEM images of AgNPs in the presence of divalent cations after 0 h (E), 48 h in dark (F) and 48 h under solar irradiation (G); the scale bar is 100 nm. A mixture of 1 mg/L ^{107}AgNPs, 1 mg/L $^{109}Ag^+$, 5 mg C/L SRHA, 40 mg/L Ca^{2+}, and 24 mg/L Mg^{2+} was treated at pH 7.4 and 30 °C.

Environmental Science: Nano Accepted Manuscript

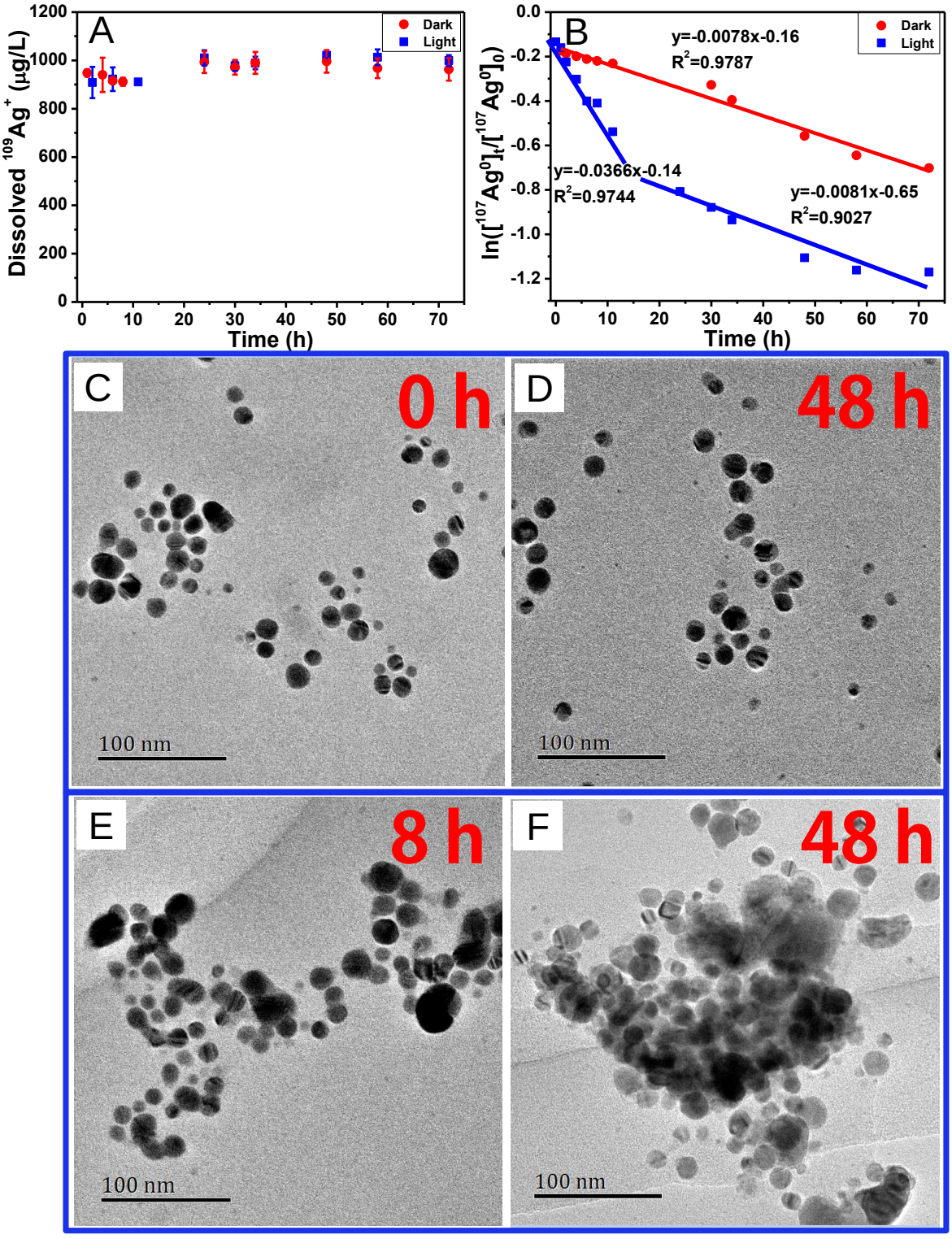

Figure 1. Transformation of AgNPs and Ag^+ in pure water. Change of dissolved $^{109}Ag^+$ over time (A); Fraction of metallic ^{107}AgNPs over time (B); and TEM images of AgNPs in the dark after 0 h (C) and 48 h (D), and in the light after 8 h (E) and 48 h (F). A mixture of 1 mg/L ^{107}AgNPs and 1 mg/L $^{109}Ag^+$ in pure water was treated at pH 7.4 and 30 °C.

Environmental Science: Nano Accepted Manuscript

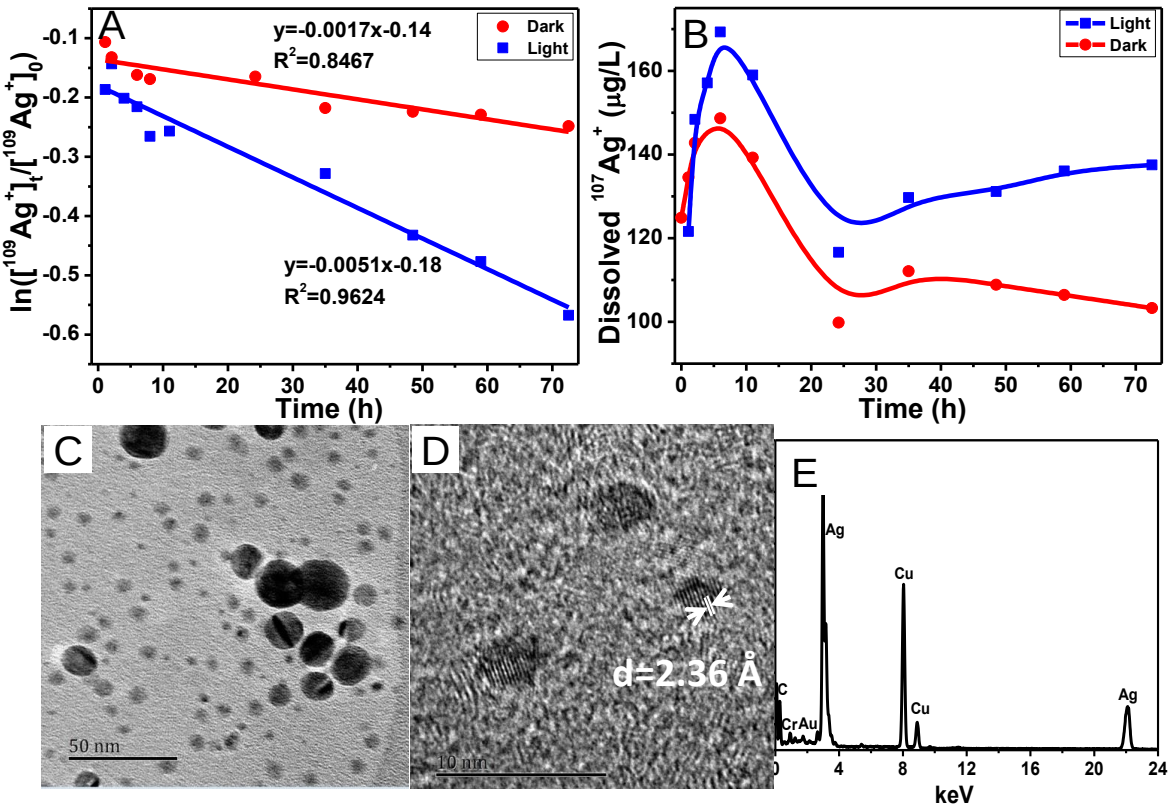

Figure 2. Transformation of AgNPs and Ag^+ in the presence of SRHA. Fraction of dissolved $^{109}Ag^+$ over time (A); Ion release kinetics of ^{107}AgNPs over time (B); and TEM image of AgNPs in the light after 24 h (C), and the HRTEM image (D) and EDS analysis (E) of the new AgNPs. A mixture of 1 mg/L ^{107}AgNPs, 1 mg/L $^{109}Ag^+$ and 5 mg C/L SRHA was treated at pH 7.4 and 30 °C.

Environmental Science: Nano Accepted Manuscript

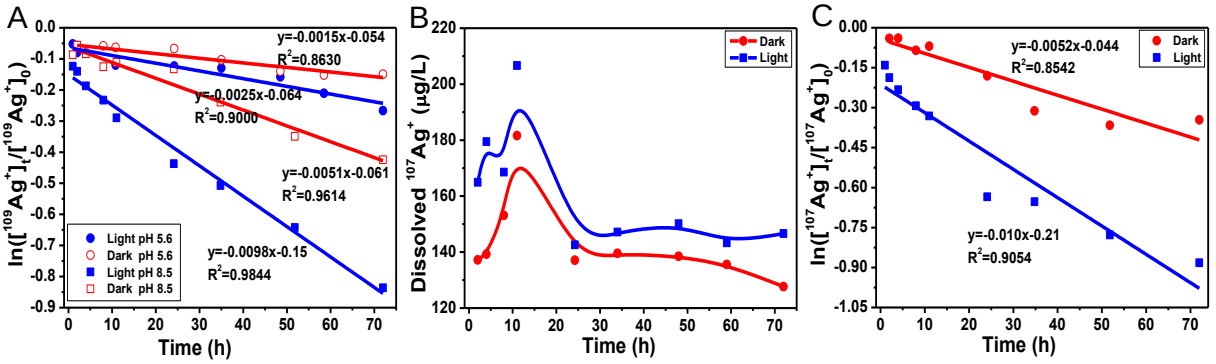

Figure 3. Fraction of dissolved $^{109}Ag^{+}$ and ion release kinetics of ^{107}AgNPs over time at different pH values. Fraction of dissolved $^{109}Ag^{+}$ at pH 5.6 and 8.5 (A), ion release kinetics of ^{107}AgNPs at pH 5.6 (B), Fraction of dissolved $^{107}Ag^{+}$ at pH 8.5 (C). A mixture of 1 mg/L ^{107}AgNPs, 1 mg/L $^{109}Ag^{+}$, and 5 mg C/L SRHA was treated at 30 °C.

Environmental Science: Nano Accepted Manuscript

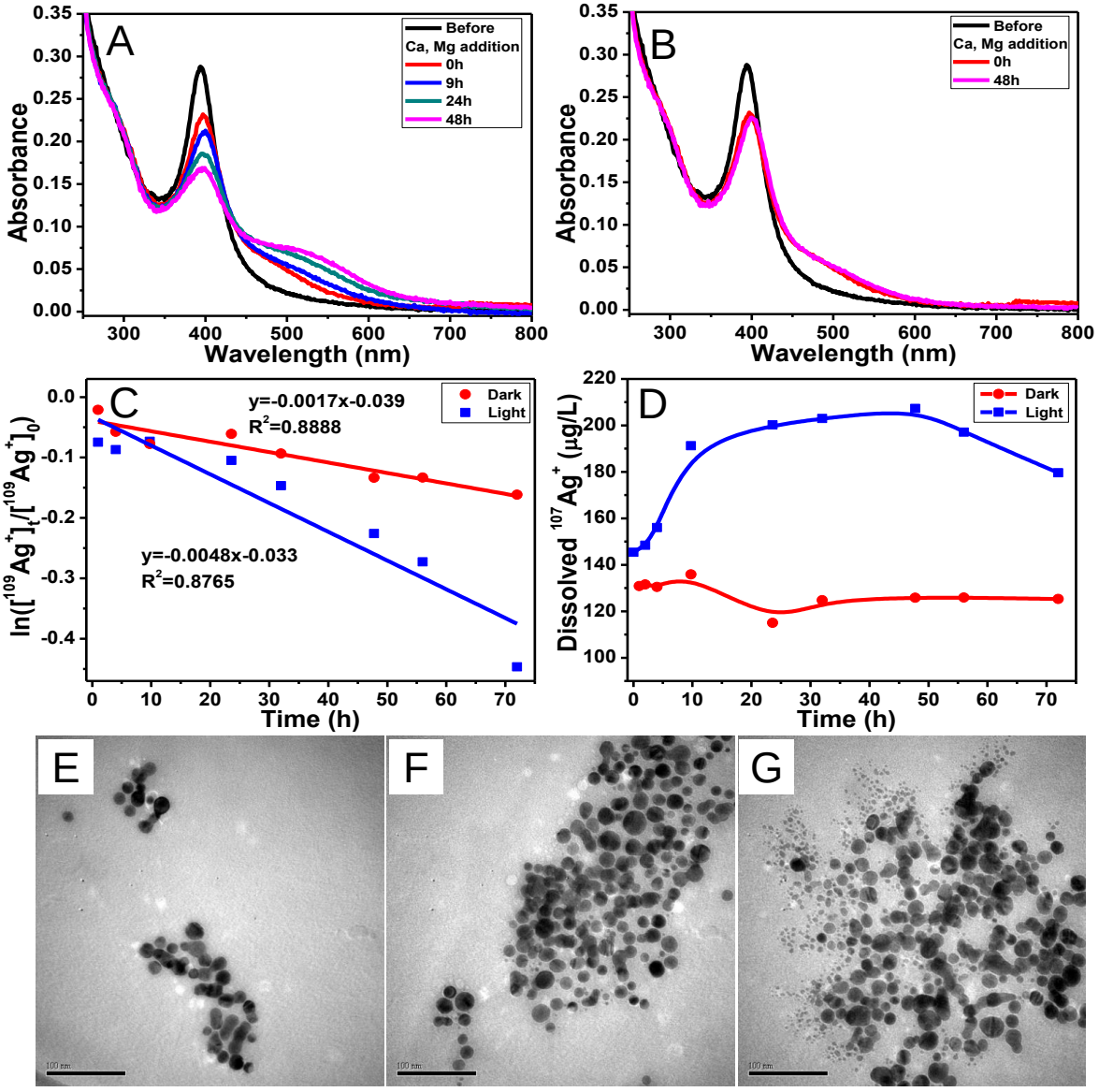

Figure 4. Impact of divalent cations on the transformation of AgNPs and Ag^{+}. UV−vis absorption spectra of AgNPs: in the light (A) and dark (B); Fraction of dissolved $^{109}Ag^{+}$ (C) and ion release kinetics of ^{107}AgNPs (D) over time; and TEM images of AgNPs in the presence of divalent cations after 0 h (E), 48 h in dark (F) and 48 h under solar irradiation (G); the scale bar is 100 nm. A mixture of 1 mg/L ^{107}AgNPs, 1 mg/L $^{109}Ag^{+}$, 5 mg C/L SRHA, 40 mg/L Ca^{2+}, and 24 mg/L Mg^{2+} was treated at pH 7.4 and 30 °C.

Environmental Science: Nano Accepted Manuscript